ARMY RESEARCH LABORATORY

Implementation of the WRF Four-Dimensional Data Assimilation Method of Observation Nudging for Use as an ARL Weather Running Estimate-Nowcast

by Robert Dumais, Steve Kirby, and Robert Flanigan

ARL-TR-6485 **June 2013**

Approved for public release; distribution is unlimited.

NOTICES

Disclaimers

The findings in this report are not to be construed as an official Department of the Army position unless so designated by other authorized documents.

Citation of manufacturer's or trade names does not constitute an official endorsement or approval of the use thereof.

Destroy this report when it is no longer needed. Do not return it to the originator.

Army Research Laboratory
White Sands Missile Range, NM 88002-5501

ARL-TR-6485 **June 2013**

Implementation of the WRF Four-Dimensional Data Assimilation Method of Observation Nudging for Use as an ARL Weather Running Estimate-Nowcast

Robert Dumais, Steve Kirby, and Robert Flanigan
Computational and Information Sciences Directorate, ARL

Approved for public release; distribution is unlimited.

REPORT DOCUMENTATION PAGE

Form Approved
OMB No. 0704-0188

Public reporting burden for this collection of information is estimated to average 1 hour per response, including the time for reviewing instructions, searching existing data sources, gathering and maintaining the data needed, and completing and reviewing the collection information. Send comments regarding this burden estimate or any other aspect of this collection of information, including suggestions for reducing the burden, to Department of Defense, Washington Headquarters Services, Directorate for Information Operations and Reports (0704-0188), 1215 Jefferson Davis Highway, Suite 1204, Arlington, VA 22202-4302. Respondents should be aware that notwithstanding any other provision of law, no person shall be subject to any penalty for failing to comply with a collection of information if it does not display a currently valid OMB control number.
PLEASE DO NOT RETURN YOUR FORM TO THE ABOVE ADDRESS.

1. REPORT DATE *(DD-MM-YYYY)*	2. REPORT TYPE	3. DATES COVERED (From - To)
June 2013	Final	July 2012–March 2013

4. TITLE AND SUBTITLE
Implementation of the WRF Four-Dimensional Data Assimilation Method of Observation Nudging for Use as an ARL Weather Running Estimate-Nowcast

5a. CONTRACT NUMBER

5b. GRANT NUMBER

5c. PROGRAM ELEMENT NUMBER

6. AUTHOR(S)
Robert Dumais, Steve Kirby, Robert Flanigan

5d. PROJECT NUMBER

5e. TASK NUMBER

5f. WORK UNIT NUMBER

7. PERFORMING ORGANIZATION NAME(S) AND ADDRESS(ES)
U.S. Army Research Laboratory
Computational and Information Sciences Directorate
Battlefield Environment Division (ATTN: RDRL-CIE-M)
White Sands Missile Range, NM 88002-5501

8. PERFORMING ORGANIZATION REPORT NUMBER
ARL-TR-6485

9. SPONSORING/MONITORING AGENCY NAME(S) AND ADDRESS(ES)

10. SPONSOR/MONITOR'S ACRONYM(S)

11. SPONSOR/MONITOR'S REPORT NUMBER(S)

12. DISTRIBUTION/AVAILABILITY STATEMENT
Approved for public release; distribution is unlimited.

13. SUPPLEMENTARY NOTES

14. ABSTRACT
The U.S. Army Research Laboratory has been performing research involving the Advanced Research Weather Research and Forecasting numerical weather prediction model and its four-dimensional (4D) data assimilation component called observation nudging.The focus has been on testing of the assimilation technique in nested and limited-area model configurations to resolve scales of 0.5–3-km grid spacing as an Army Weather Running Estimate-Nowcast tool. The tool would provide a rapid-update cycling application for generating short-range forecast/nowcast updates at storm-scale resolutions. The observation nudging method is considerably less computationally expensive than the suite of more advanced 4D-variational and ensemble Kalman filter data assimilation systems used at large operational centers. It is based upon the same general principles of the Kalman gain theory as are the variational and ensemble methods and has been shown to be an effective method of assimilating asynoptic meteorological observations into high-resolution models. Focus here is upon model configuration and the steps required to generate the hourly cycled model runs. Special weather observations collected over Yuma Proving Ground, AZ, during November 30–December 01, 2007, were ingested into the system for a case study application example. However, this report's intent is to focus upon the methodology rather than verification of the meteorology.

15. SUBJECT TERMS
wrf, numerical, model, assimilation, cycling, nudging, meteorology

16. SECURITY CLASSIFICATION OF:			17. LIMITATION OF ABSTRACT	18. NUMBER OF PAGES	19a. NAME OF RESPONSIBLE PERSON
a. REPORT	b. ABSTRACT	c. THIS PAGE			Robert Dumais
Unclassified	Unclassified	Unclassified	UU	24	19b. TELEPHONE NUMBER (*Include area code*) (575) 678-4650

Standard Form 298 (Rev. 8/98)
Prescribed by ANSI Std. Z39.18

Contents

List of Figures

List of Tables

Acknowledgments

The U.S. Air Force Weather Agency (AFWA) provided funding and guidance to the U.S. Army Research Laboratory (ARL) to provide this Numerical Weather Prediction (NWP) model research.

INTENTIONALLY LEFT BLANK.

1. Introduction

The U.S. Army Research Laboratory (ARL) Battlefield Environment Directorate (BED) has been performing research involving the Advanced Research Weather Research and Forecasting (ARW-WRF) numerical weather prediction model (Skamarock et al., 2008) and its four-dimensional (4D) data assimilation (FDDA) component called observation or "station" nudging (Liu et al., 2005, 2007; Reen and Stauffer, 2010). Hereafter in this report, ARW-WRF will simply be referred to as WRF. The focus has been on testing of the FDDA technique in a nested and limited-area WRF configuration to resolve scales of 0.5–3-km grid spacing as an Army Weather Running Estimate-Nowcast (WRE-N) tool. The WRE-N will provide a rapid-update cycling application for generating short-range forecast/nowcast updates of local battlefield weather conditions at storm-scale resolutions. For use as a WRE-N, ARL has been testing various aspects of the WRF involving model vertical resolution, time-stepping, microphysics, planetary boundary layer (PBL) physics, turbulence parameterization, and observation nudging data assimilation. Some of these test results are discussed in Raby et al., 2011.

A popular and relatively inexpensive (in terms of computation) form of intermittent atmospheric data assimilation for meso and synoptic scales is that of the three-dimensional variational (3DVAR) (Barker et al., 2003), requiring temporal interpolation of observations to fixed analysis times. However, an intermittent data assimilation scheme is more likely to induce initial shock into the model (unless techniques such as digital filter initialization are applied) and to be less effective for asynoptic and high-frequency observation networks. Some simple methods such as First Guess at Appropriate Time (Lee and Barker, 2005) have been developed to better incorporate the differences between observation and model analysis times within the innovation calculation of 3DVAR schemes. Other more elaborate methods based upon multigrid methods have been applied to 3DVAR for more accurate capturing of temporal information in the observations (Xie et al., 2011) despite the intermittent nature of the data assimilation approach.

This report focuses instead upon the application and testing of the WRF FDDA method. The continuous atmospheric data assimilation technique of observation nudging (Deng et al., 2009; Liu et al., 2005) is considerably less expensive, computationally, than the more advanced 4D-variational continuous method used in the WRF Data Assimilation (DA) package (Huang et al., 2009) or the ensemble Kalman filter approach (Zupanski et al., 2008). It is also based upon the same general principles of the Kalman gain theory as are the variational and ensemble methods (Liu et al., 2005). The technique of observation nudging has been shown to be a viable and effective method of assimilating asynoptic meteorological observations into high-resolution atmospheric models for improving short-range forecasting (Deng et al., 2009). ARL seeks to use this method in its WRE-N as the tool for assimilating forward-area asynoptic battlefield meteorological observations, which may not get regularly ingested into the U.S. Air Force

Weather Agency (AFWA) operational WRF 3DVAR system (Surmeier and Wegiel, 2004). Surface, upper-air radiosonde/dropsonde, profiler, tethered, and aircraft direct (or convertible into direct) observations of wind, temperature, moisture, and pressure are the current focus in WRE-N. Frequently updated "running estimates" of local battlefield weather conditions (i.e., 4D weather cubes) can be used in decision aid algorithms and aviation routing tools, which in turn can be used by commanders for mission execution planning purposes.

In this report, we focus mostly on the model configuration and the steps required to generate hourly cycled WRF FDDA model runs. We also give a brief example in applying the method for a case study over the Yuma Proving Ground (YPG), AZ. Special asynoptic weather observations (surface and radiosonde) collected over YPG from November 30 to December 01, 2007, were ingested into the system for that case example. These observations were taken in support of ScanEagle unmanned aerial system testing and are appropriate for applying and testing the FDDA cycling method at fine scales. However, this report's intent is not to focus upon the verification of the meteorology of this specific case. Rather, it is to describe the general methodology.

2. WRF Model Configuration

Spatially, a 3- and 1-km double-nest strategy is used, with 171 × 171 grid point dimensions on the outer (510 km × 510 km) and 103 × 103 grid dimensions on the inner (102 km × 102 km) nests, respectively. The nests are one-way interactive. To provide the high-resolution initial atmospheric and surface conditions, along with the time-dependent lateral boundary conditions for the 3-km outer nest, the National Centers for Environmental Prediction's North American Model (NAM) 218 grids (Rogers et al., 2009) are used. The NAM grids are nominally at about 12-km horizontal grid spacing, so they maintain a good scaling ratio with the 3-km outer nest. The size and resolution of the outer nest, along with that of the inner nest, are sufficiently small enough to remain computationally viable on a small cluster or high-end multiprocessor workstation, yet are large enough so that model solutions near the domain center remain reasonably buffered from NAM lateral boundary condition errors throughout the short-range cycling forecast period. Frequent data assimilation cycling (such as here every hour), use of short continuous self-cycling periods (12–24 h), and short model forecast extent per cycle (3–6 h) all work toward limiting the damage from any potential model errors introduced through the external lateral boundary conditions. In the vertical, 90 levels are used with the lowest model half-level at about 25 magl. This offers greater vertical resolution for the current YPG experiment than the typical 60 levels used for WRE-N. The vertical grid is staggered log-linearly, so that maximum resolution is maintained within the boundary layer. The specifications of the WRF nests, along with a control set of namelist (model control) options are shown in table 1.

Table 1. Namelist options for WRF control run used in this model study.

Namelist Parameter	Option Selected
Short wave radiation scheme	Dudhia scheme
Long wave radiation scheme	RRTM[a]
Explicit moist microphysics	WSM 5-class[b]
Cumulus parameterization	None on both nests
PBL scheme	Quasi-normal scale elimination
Surface layer	Quasi-normal scale elimination
Land surface scheme	NOAH[c] land-surface model
Time step (sec) to grid-spacing (km) ratio	3:1
Horizontal sub grid diffusion	2nd order on coordinate surfaces
Sub grid turbulence closure	Horizontal Smagorinsky 1st order closure
Number of vertical terrain-following levels	90
Vertical velocity damping	Yes
Feedback (two-way interactive)	No
Nesting	Yes
Terrain slope/shadow	Yes
FDDA	Yes
Nudging strength for T,q,u,v	1.0 × 10**–3 s

[a] Rapid Radiative Transfer Model.
[b] WRF Single Moment 5-Class.
[c] Nationwide Operational Assessment of Hazards.

3. Observation Nudging FDDA

Station or observation nudging is a means to guide the model solution toward the observations rather than toward analyses and is implemented by adding non-physical nudging terms to the model predictive equations. The method is implemented through an extra tendency term in the nudged variable's equation:

$$\frac{\partial \Theta}{\partial t} = F(\Theta) + G_\Theta W_\Theta (\tilde{\Theta}_0 - \Theta), \quad (1)$$

where $F(\Theta)$ represents the normal tendency terms due to physics/advection, G_Θ is a timescale controlling the nudging strength, and W_Θ is an additional weight in time or space (x,y,P) to limit the nudging as described more in the following. In addition, $\tilde{\Theta}_0$ is the observed value, and Θ is the model value spatially interpolated to the location of the observation.

These terms force the model solution at each grid point toward the observations, in proportion to the difference (innovation) between the data and the model solution. Each observation is ingested into the model at its observed time and location, with various user-defined space and time weights. Several recent papers have examined the impact of assigning appropriate horizontal and vertical radii of influence for observations based upon factors such as model nest resolution, boundary layer stability, terrain, synoptic forcing, and land surface heterogeneities (Gaudet et al., 2009; Reen and Stauffer, 2010; Yu et al.; 2007; Pattantyus and Dumais, 2011). It appears from

such studies that for different grid resolutions, climatic/geographical locations, and meteorological and boundary layer conditions, that different rules of thumb may need to be applied for assessing weights and radii of influence as applied to the observation nudging.

4. FDDA Cycling Methodology

In a general sense, the concept of cycling involves a repeating process of model "self correction" through the assimilation of weather observations. On fine scales such as the meso-beta and meso-gamma, the continuous FDDA method has been shown to be a useful methodology for cycling, especially when a dense asynoptic observation network exists (Deng et al., 2009). In this case study we used a self-cycling period (i.e., period between each new cold start) spanning between 09 Coordinated Universal Time (UTC) on November 30 and 00 UTC on 01 December. Since a 1-h cycling frequency is applied, a total of 16 cycles are executed throughout the aforementioned period. For each cycle, a 3-h FDDA "pre-forecast" period is followed by a 3-h free-forecast period. So, for any analysis hour t_0, the model actually integrates between t_0–3 h and t_0+3 h.

The initial model cycle was tagged as 09 UTC, which means it was actually run for the period between 06 UTC (FDDA between 06 and 09 UTC) and 12 UTC (3-h forecast 09–12 UTC). At the start of the first cycle's integration period (i.e., 06 UTC), the "cold start" initial conditions were provided by the 06 UTC forecast cycle grids of the NAM. All time-dependent lateral boundary tendencies required out to the last forecast hour of the final cycle were also provided by the 06 UTC NAM forecast grids. In other words, for the final 00 UTC on the 01 December cycle, the 21-h forecast from the 06 UTC 30 November NAM is used to provide the 3-km nest its lateral boundary tendencies at 03 UTC 01 December.

The second hourly cycle tagged as 13 UTC on 30 November is executed in similar fashion; except, that the initiation began at 10 UTC on 30 November using the 10 UTC 30 November WRF fields produced from the previous cycle's run. In this sense, all remaining hourly cycles use WRF initial conditions produced from the previous cycle.

This sort of “self-cycling” in an operational mode would proceed until the next “cold start” initiation from a new NAM forecast data set usually 12–24 h later based upon the WRE-N configuration.

The WRF namelist option called *restart* is used to perform the cycling. First, the WRF Preprocessor System (WPS) and Real programs are executed as if a single continuous forecast integration between 06 UTC November 30 and 03 December 01 is desired (creating *wrfbdy** and *wrfinp** files, which remain static for the duration of the cycling period thereafter). The *restart* method in WRF generates special output files at each model integration hour throughout each forecast cycle. This is all accomplished within the WRF namelist by setting parameter “restart_interval” to 60 (units in minutes), and the “restart interval” parameter must be set less than or equal to the model integration length per cycle (for the YPG example, this is 6 h). When the model reaches the time to write a new *restart* file, a file named *wrfrst_d<domain>_<date>* is written. The date string represents the time for which the *restart* file is valid and it is essentially the full model state saved at that point in time.

Just prior to the start of each *restart* run (i.e., a new hourly cycle), the namelist file is edited again so that the new model integration start and end times are updated. The start and end times for the FDDA are also incremented by 60 min in the namelist file. The new cycle then initiates using the *wrfrst_d<domain>_<date>* files valid at the 1-h integration point of the previous cycle. Essentially, the model just picks up where it left off at 1 h into the last cycle’s integration. In addition, FDDA is applied for the first 3 h of integration using the most current observation data. After the FDDA period, the last 3 h of each cycle run is purely prognostic. This process continues until all cycles, out to that of 00 UTC 01 December, are executed.

A second method besides *restart* for implementing cycling using the WRF FDDA is based using the boundary condition update software that is part of the WRFVAR software package. It is also the method used for cycling using the WRF 3DVAR approach. This method has been developed at ARL (referred to here as *cycling*) and was tested using the YPG datasets. This software (1) adjusts the *wrfinp** initial condition files by leveraging the 1-h integrated atmospheric fields of the last cycle; (2) similarly, adjusts the static surface-state fields such as soil temperature, snow cover, sea surface temperature, and skin temperature; and (3) adjusts the lateral boundary condition tendencies within *wrfbdy** by using the new *wrfinp** data. A skew-T comparing the YPG radiosonde of 2007 December 1, 00 UTC against the WRF *cycling* (via boundary condition update) and WRF *restart* output is shown in figure 1. Except for a layer from about 350 to 260 mb, where the cycling method shows a saturated layer, the temperature profiles for the cycling and restart methods are quite similar. It should be noted that although the *restart* runs used 90 vertical levels for the YPG cycling, the *cycling* runs kept to the more traditional 60 vertical levels used in WRE-N. This difference can be seen in the skew-T plot. Also, results below are shown for the 3-h forecast based off of the 21 UTC November 30 cycle. Thus, only observations up to 21 UTC (including a 21 UTC YPG radiosonde) were assimilated in producing these results. The 1-h cycling process used for the YPG study is shown in figure 2.

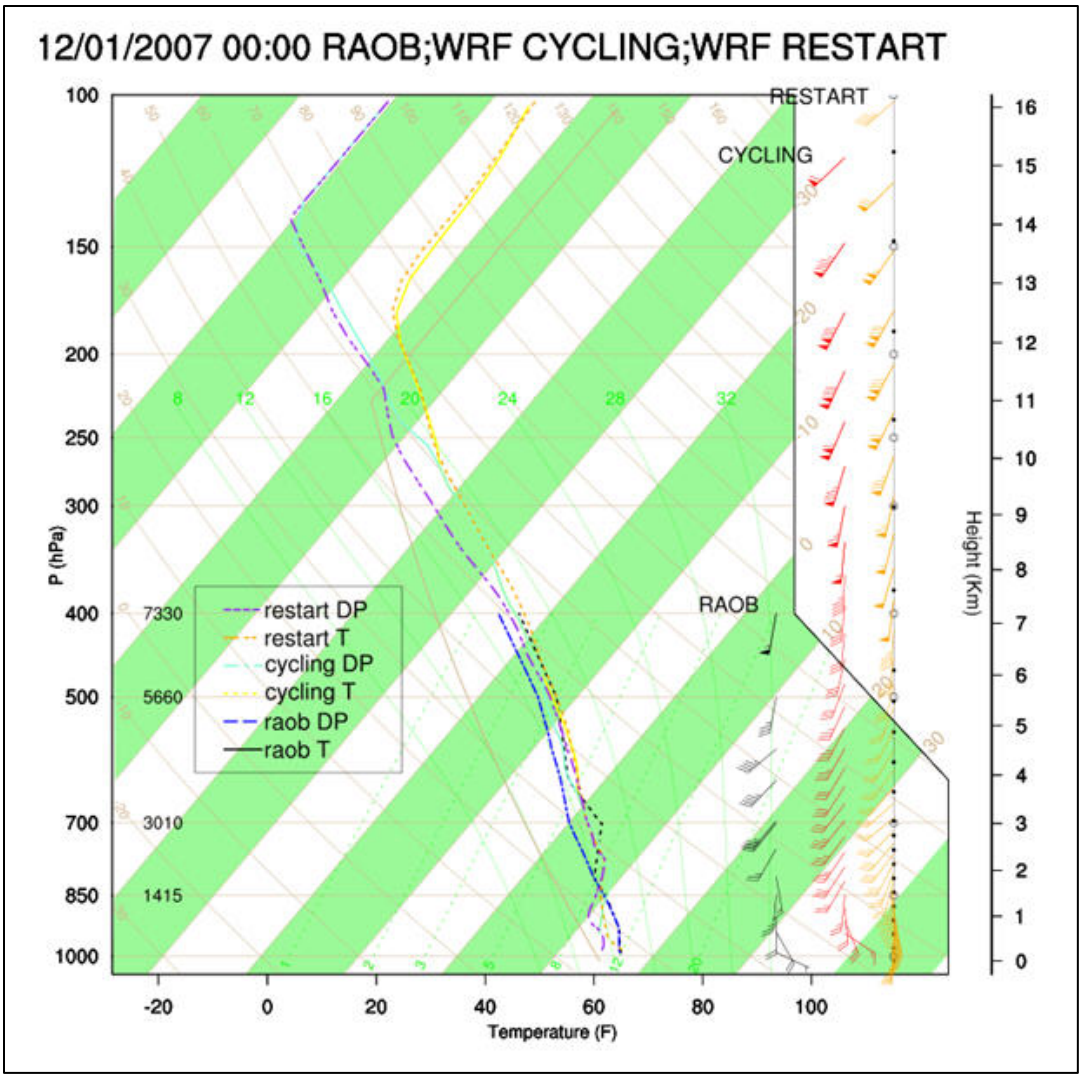

Figure 1. Comparison of WRF cycling and restart methods with RAOB* data.

* RAwinsonde OBservation program.

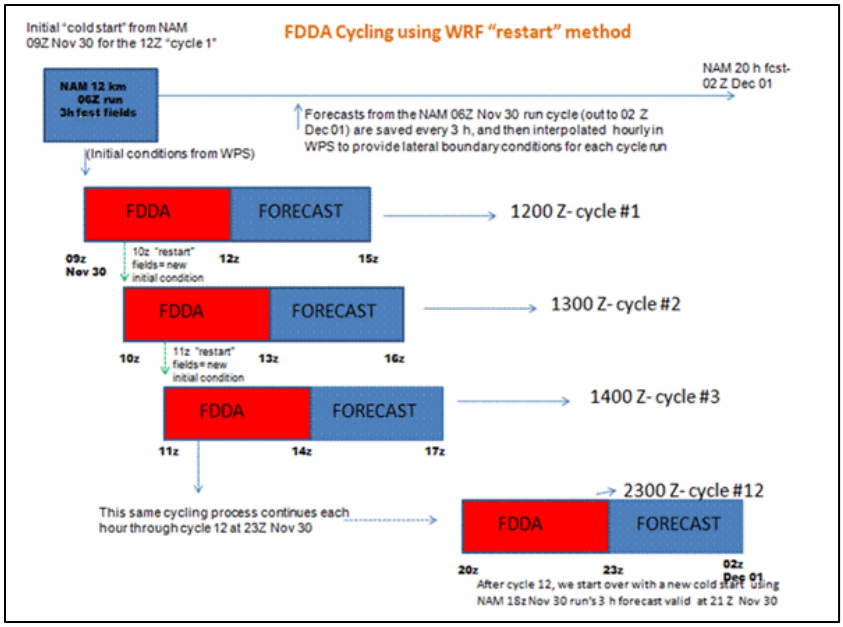

Figure 2. FDDA with WRF restart method.

While these two cycling methodologies look to generate comparable results, this second method that employs boundary condition updates appears clumsier and less suitable for use with WRF FDDA than does *restart*, especially for shorter "between cold start" self-cycling periods. In addition, many groups that apply FDDA in a cycling mode appear to use *restart* as the method of choice. This report focuses only on results using the *restart* method from here forward.

5. YPG Case of November 30, 2007

During late November and early December of 2007, a series of field experiments were conducted over the YPG in support of ScanEagle unmanned aerial system flight tests. ARL participated in these by supplying on-site weather forecasting support, which included remotely running the high-resolution WRF model (without FDDA at that time). In addition, YPG personnel maintained, operated, and archived a set of local surface mesonet observations (including a few meteorological towers) in addition to numerous asynoptic radiosonde releases daily. The local YPG weather observations from 30 November were used to test the WRF observation nudging FDDA applied in an hourly cycling mode.

The overall synoptic conditions for this day are shown in figures 3 and 4, for 12 UTC 30 November and 00 UTC 01 December, respectively. By late afternoon, strong subtropical low- and midlevel moisture advection from the south was occurring over southeast California and southwest Arizona. This was ahead of an approaching upper-level trough in the subtropical jet stream. Additionally, a strong short-wave in the polar jet stream off the California coast was

trying to phase with the trough in the subtropical jet. All of this led to a period of afternoon and early evening upper-level diffluence, vertical wind shear, positive vorticity advection, and slightly unstable stability indices to support widespread precipitation and convection across the area. Table 2 provides the radiosonde data collected from the 00 UTC 01 December radiosonde at YPG, showing a deep moist atmospheric column all the way up through 400 mb. Most stability indices were weakly supportive of convection at this time.

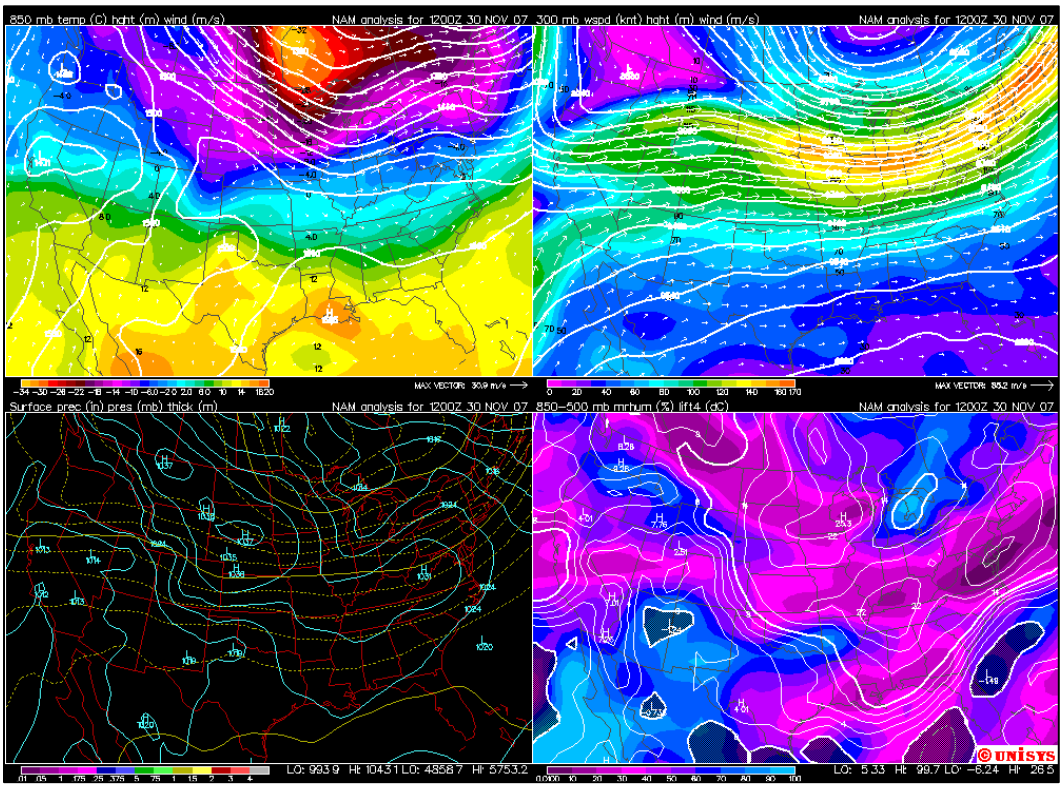

Figure 3. Upper level and surface conditions as produced by the NAM analysis and valid at 12 UTC 30 November. (Figure 3 is from UNISYS*.)

*UNISYS is a trademark of Unisys Corporation.

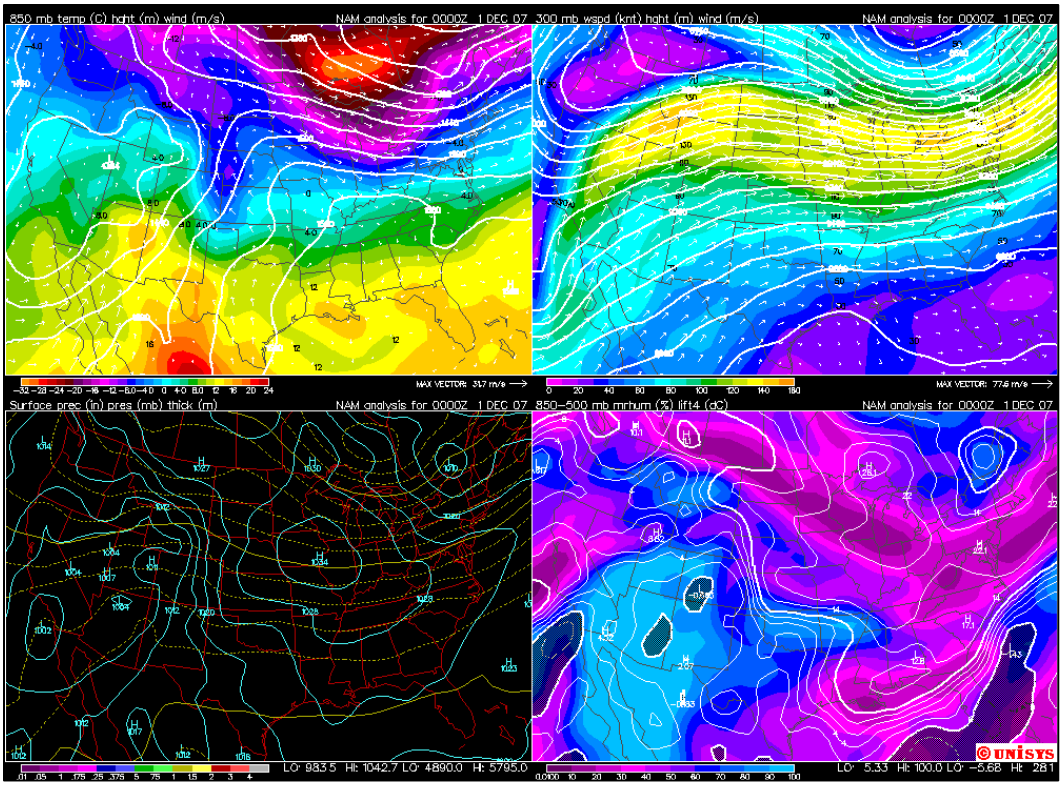

Figure 4. Upper level and surface conditions as produced by the NAM analysis and valid at 00 UTC 01 December. (Figure 4 is from UNISYS.*)

Table 2. Radiosonde from YPG, 00 UTC December 01, 2006.

Radiosonde 74004: Observations at 00 UTC 01 December 2007										
PRES (hPa)	**HGHT (m)**	**TEMP (°C)**	**DWPT (°C)**	**RELH (%)**	**MIXR (g/kg)**	**DRCT (degree)**	**SKNT (knot)**	**THTA (K)**	**THTE (K)**	**THTV (K)**
1000.0	41	—	—	—	—	—	—	—	—	—
900.0	231	16.4	16.3	99	11.91	115	5	290.4	324.1	292.5
979.6	305	16.0	15.9	99	11.76	145	14	290.9	324.2	292.9
937.7	610	14.5	14.5	100	11.16	150	21	293.0	324.9	294.9
925.0	705	14.0	14.0	100	10.98	175	19	293.6	325.1	295.6
902.3	914	12.8	12.8	100	10.37	180	19	294.5	324.4	296.3
870.1	1219	11.1	11.0	99	9.53	185	24	295.8	323.5	297.5
850.0	1415	10.0	9.8	99	9.02	185	23	296.6	323.0	298.2
813.0	1784	7.4	7.4	100	8.00	172	16	297.6	321.3	299.1
808.6	1829	7.2	7.1	99	7.90	170	15	297.9	321.3	299.4
779.0	2134	6.2	5.3	94	7.22	185	17	300.1	321.7	301.4
750.6	2438	5.2	3.5	88	6.58	210	23	302.2	322.1	303.4
723.2	2743	4.2	1.6	83	5.99	205	32	304.3	322.7	305.4
701.0	2998	3.4	0.1	79	5.53	219	37	306.1	323.2	307.1
700.0	3010	3.2	0.0	80	5.50	220	37	306.0	323.1	307.0
696.7	3048	2.9	–0.2	80	5.45	220	37	306.1	323.0	307.1
645.7	3658	–1.7	–3.2	90	4.70	220	43	307.6	322.4	308.4
625.0	3920	–3.7	–4.5	94	4.40	224	44	308.2	322.1	309.0
597.8	4267	–5.4	–6.4	93	3.99	230	45	310.2	322.9	310.9

*See footnote on page 8.

Table 2. Radiosonde from YPG, 00 UTC December 01, 2006 (continued).

Radiosonde 74004: Observations at 00 UTC 01 December 2007										
PRES (hPa)	**HGHT (m)**	**TEMP (°C)**	**DWPT (°C)**	**RELH (%)**	**MIXR (g/kg)**	**DRCT (degree)**	**SKNT (knot)**	**THTA (K)**	**THTE (K)**	**THTV (K)**
574.9	4572	–6.8	–8.1	91	3.64	230	46	311.9	323.7	312.6
552.8	4877	–8.3	–9.7	90	3.32	210	33	313.7	324.6	314.3
500.0	5660	–12.1	–14.0	86	2.60	190	34	318.2	327.0	318.7
471.7	6096	–15.0	–16.9	85	2.17	195	35	320.0	327.4	320.4
400.0	7330	–23.1	–25.2	83	1.24	190	54	324.9	329.4	325.1

Doppler radar composites from 00 UTC 01 December (figures 5 and 6) show that much of southeast California, central and southern Arizona were under a wide area of precipitation including isolated convection. The model-derived composite reflectivity plots in figures 5 and 6 both compare reasonably well in terms of the gross features of this event captured by radar. However, the model run that used the *restart* cycling FDDA approach (as opposed to the cold start) subjectively seems to have done a somewhat better job of reproducing (1) the reduced precipitation area over northwest Arizona; and (2) the heavier precipitation area over the central Mogollon Rim.

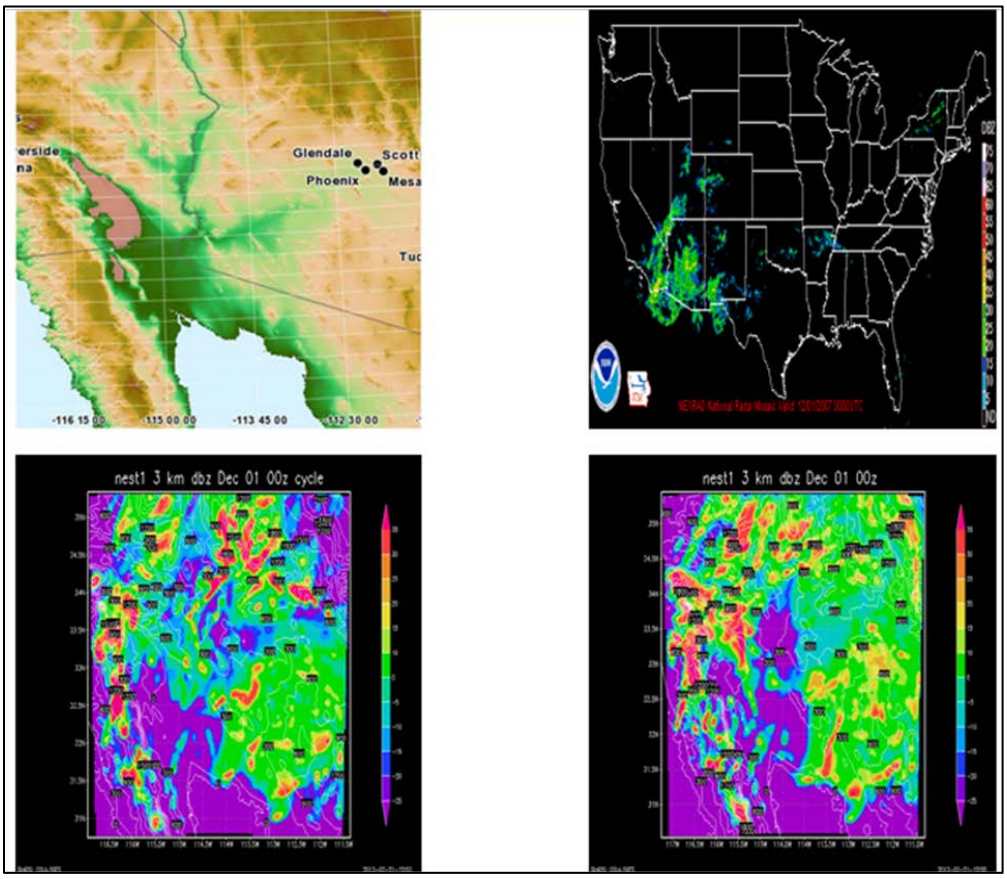

Figure 5. Domain 1 (3 km) region in upper left; U.S. Doppler radar composite at 00 UTC 01 December 2007, in upper right; domain 1 model composite reflectivity (with FDDA) at 00 UTC 01 December 2007, in bottom left; domain 1 model composite reflectivity (no FDDA) at 00 UTC 01 December 2007, in bottom right.

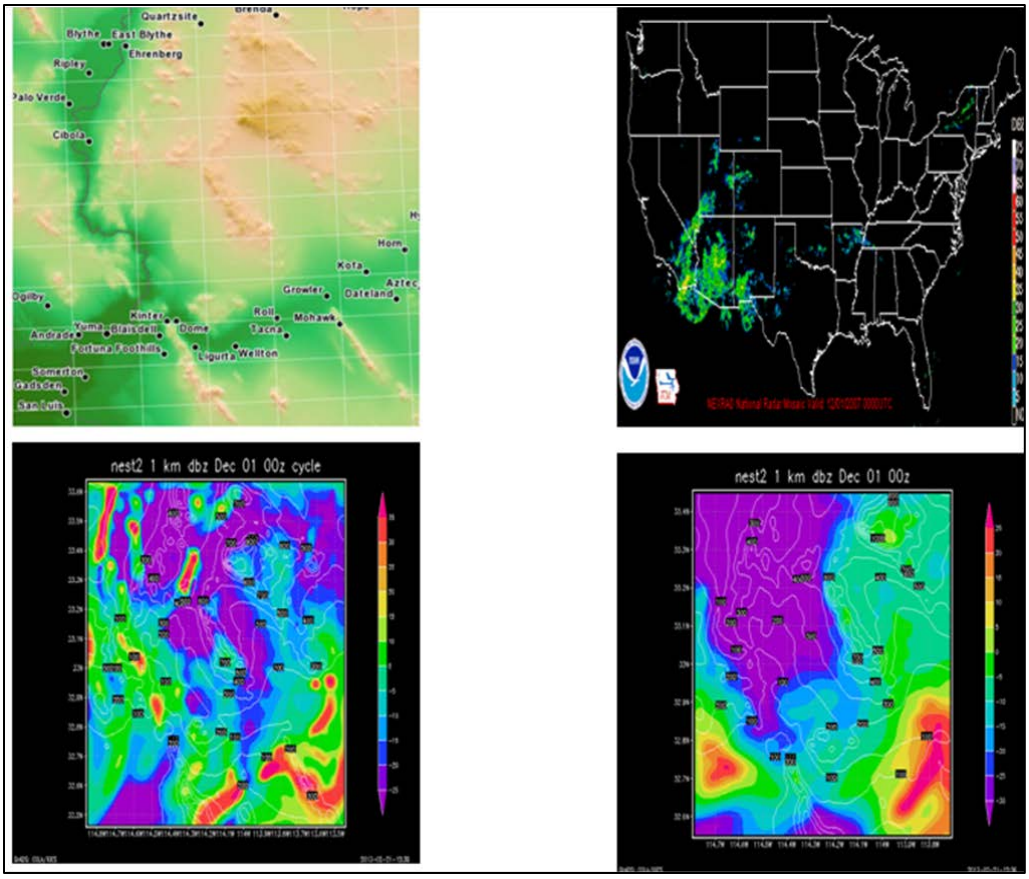

Figure 6. Domain 2 (1 km) region in upper left; U.S. Doppler radar composite at 00 UTC 01 December 2007, in upper right; domain 2 model composite reflectivity (with FDDA) at 00 UTC 01 December 2007, in bottom left; domain 2 model composite reflectivity (no FDDA) at 00 UTC 01 December 2007, in bottom right.

6. Summary

The goal of this report was to describe an approach being developed and tailored at ARL that is based on the mesoscale WRF model and its observation nudging FDDA that would provide the Army with a short-range "nowcast" system capable for predicting scales resolvable at as fine as 1-km grid spacing. This system is called the WRE-N. The hope is that the WRE-N can be tailored in a fashion that would make it amenable to running on computer hardware likely to be available tactically at a Distributed Common Ground System-Army (DCGS-A) or Artillery unit.

The majority of this report describes the reasoning behind the model's limited-area nesting strategy (along with showing physics options used), the theory of observation nudging FDDA, and the concept of rapid-update cycling using WRF and FDDA. Although two different methods were tested to perform cycling of the WRF-FDDA system, only the method referred to as "*restart*" was focused upon. A very brief discussion of a case study event over YPG, AZ, using

the "*restart*" cycling approach at an hourly cycle rate demonstrated that the system executes properly and has potential to add short-range forecast benefit to the Army. Further studies are ongoing that are now focusing on verification of the system for various case events based on observed ground truth, along with fine-tuning of the weights used in the observation nudging algorithm. In addition, an improved observation quality control system is being developed for the system front-end. For verification, the NCAR Model Evaluation Tool (MET) is being used. Beyond simple point-based standard statistical metrics, research is ongoing at ARL toward using the object-oriented verification tools of MET, which will allow for a more effective verification of high-resolution model performance in the future.

7. References

Barker, D. M.; Huang, W.; Guo, Y. -R.; Bourgeois, A. *A Three-Dimensional Variational (3DVAR) Data Assimilation System for Use With MM5*; NCAR/TN-453+STR; National Center for Atmospheric Research (NCAR), Mesoscale and Microscale Meteorology (MMM) Division: Boulder, CO, 2003, p 68.

Deng, A.; Stauffer, D.; Gaudet, B.; Dudhia, J.; Bruyere, C.; Wu, W.; Vandenberghe, F.; Liu, Y.; Bourgeois, A. *Update on WRF-ARW End-to-End Multiscale FDDA System*. The 10th Users' Workshop, National Center for Atmospheric Research (NCAR), Boulder, CO, June 23–26, 2009.

Gaudet, B. J.; Stauffer, D. R.; Seaman, N. L.; Deng, A.; Pleim, J. E.; Gilliam, R.; Schere, K.; Elleman, R. A. *Modeling Extremely Cold Stable Boundary Layers Over Interior Alaska using a WRF FDDA System*. The 13th Conference on Mesoscale Processes, American Meteorological Society, Salt Lake City, UT, August 17–20, 2009.

Huang, X. Y.; Xiao, Q.; Barker, D. M.; Zhang, X.; Michalakes, J.; Huang W.; Henderson, T.; Bray, J.; Chen, Y.; Ma, Z.; Dudhia, J.; Guo, Y.; Zhang, X.; Won, D. J.; Lin, H. C.; Kuo, Y. H. Four-Dimensional Variational Data Assimilation for WRF: Formulation and Preliminary Results. *Mon. Wea. Rev.* **2009**, *137*, 299–314.

Lee, M. -S.; Barker, D. M. Preliminary Tests of First Guess at Appropriate Time (FGAT) with WRF 3DVAR and WRF Model. *Journal of the Korean Meteorological Society* **2005**, *41*, 495–505.

Liu, Y.; Bourgeois, A.; Warner, T.; Swerdlin, S.; Hacker, J. *Implementation of Observation Nudging-Based FDDA Into WRF for Supporting ATEC Test Operations*. The 6th WRF/15th MM5 Users' Workshop, Session 10.7, National Center for Atmospheric Research (NCAR), Boulder, CO, 2005.

Liu, Y.; Bourgeois, A.; Warner, T.; Swerdlin, S. *An Observation Nudging-Based FDDA for ARW-WRF for Mesoscale Data Assimilation and Forecasting*. The 4th Symposium of Space Weather, 87th AMS Meeting, San Antonio, TX, January 13–18, 2007.

Pattantyus A.; Dumais, R. *Optimizing Strategies for an Observation Nudging-Based Four-Dimensional Data Assimilation Forecast Approach with WRF-ARW*. ARL Summer SEAP Symposium, Aberdeen, MD, August 2011.

Raby, J.; Passner, J.; Brown, R.; Raby, Y. *Traditional Statistical Measures Comparing Weather Research and Forecast Model Output to Observations Centered Over Utah*; ARL-TR-5422; U.S. Army Research Laboratory: White Sands Missile Range, NM, January 2011, p 314.

Reen, B. P.; Stauffer, D. R. Data Assimilation Strategies in the Planetary Boundary Layer. *Bound.-Layer Meteor*., **2010**, 137, 237–269.

Rogers, E.; DiMego, G.; Black, T.; Ek, M.; Ferrier, B.; Gayno, G.; Janjic, Z.; Lin, Y.; Pyle, M.; Wong, V.; Wu, W-S.; Carley, J. *The NCEP North American Mesoscale Modeling System: Recent Changes and Future Plans*. The 23rd Conference on Weather Analysis and Forecasting/19th Conference on Numerical Weather Prediction, American Meteorological Society, Omaha, NE, June 1–5, 2009.

Skamarock, W. C.; Klemp, J. B.; Dudhia, J.; Gill, D. O.; Barker, D. M.; Duda, M. G.; Huang, X-Y; Wang, W.; Powers, J. G. *A Description of the Advanced Research WRF Version 3*. NCAR/TN-475=STR; National Center for Atmospheric Research (NCAR), Mesoscale and Microscale Meteorology (MMM) Division: Boulder, CO, June 2008, p 113.

Surmeier, M. T.; Wegiel, J. W. *On the Optimization of the Air Force Weather Weapon System's Next Generation Mesoscale Numerical Weather Prediction Model: The Weather Research and Forecast Model (WRF).* HQ Air Force Weather Agency (AFWA), 20th Conference on Weather Analysis and Forecasting/16th Conference on Numerical Weather Prediction, 84th American Meteorological Society Meeting, Seattle, WA, January 10–16, 2004.

Xie, Y.; Koch, S.; McGinley, J.; Albers, S.; Bieringer, P. E.; Wolfson, M.; Chan, M. A Space—Time Multiscale Analysis System: A Sequential Variational Analysis Approach. *Mon. Wea. Rev*. **2011**, *139*, 1224–1240.

Yu, W.; Liu, Y.; Warner, T. *An Evaluation of 3DVAR, Nudging-Based FDDA and a Hybrid Scheme for Summer Convection Forecasting Using WRF-ARW Model*. The 18th Conference on Numerical Weather Prediction, American Meteorological Society, Park City, UT, June 25–29, 2007, p 5.

Zupanski, M.; Navon, I. M.; Zupanski, D. The Maximum Likelihood Ensemble Filter as a Non-Differential Minimization Algorithm. *Q.J.R. Meteor. Soc*. **2008**, *134*, 1039–1050.

List of Symbols, Abbreviations, and Acronyms

3DVAR	three-dimensional variational
4D	four-dimensional
AFWA	U.S. Air Force Weather Agency
ARL	U.S. Army Research Laboratory
ARW-WRF	Advanced Research Weather Research and Forecasting
BED	Battlefield Environment Directorate
DA	Data Assimilation
DCGS-A	Distributed Common Ground Sysem-Army
FDDA	four-dimensional data assimilation
MET	Model Evaluation Tool
NAM	North American Model
NOAH	Nationwide Operational Assessment of Hazards
NWP	Numerical Weather Prediction
PBL	planetary boundary layer
RAOB	RAwinsonde OBservation program
RRTM	Rapid Radiative Transfer Model
UTC	Coordinated Universal Time
WPS	WRF Preprocessor System
WRE-N	Weather Running Estimate-Nowcast
WSM 5-Class	WRF Single Moment 5-Class
YPG	Yuma Proving Ground

No. of Copies	Organization
1 (PDF)	DEFENSE TECHNICAL INFORMATION CTR DTIC OCA
2 (PDFs)	DIRECTOR US ARMY RESEARCH LAB RDRL CIO LL IMAL HRA MAIL & RECORDS MGMT
1 (PDF)	GOVT PRINTG OFC A MALHOTRA
3 (PDFs)	DIRECTOR US ARMY RESEARCH LAB RDRL CIE M R DUMAIS S KIRBY R FLANIGAN